"Snapping" torsional response can lead to a worsening crack situation

by Donald E. Bently
Chairman and Chief Executive Officer
Bently Nevada Corporation
President, Bently Rotor Dynamics Research Corporation

and Paul Goldman, Ph.D
Research Scientist
Bently Nevada Corporation

and Agnes Muszynska, Ph.D
Senior Research Scientist
Bently Rotor Dynamics Research Corporation

Torsional vibrations, due to nonlinear coupling of the torsional and lateral modes, are responsible for a "snapping" action of the rotor, which can intensify crack propagation. These vibrations can also initiate a rotor crack in the area of stress concentration, and can be the cause of coupling failure. The torsional vibrations are due to nonlinear coupling of the torsional and lateral modes, excited by unbalance and the radial sideload force together with the rotating anisotropy of the rotor. High torsional response has the frequency of 1X and 2X, and the snapping action occurs when the rotative speed coincides with the lowest torsional natural frequency, or half of it (the 1X and 2X torsional resonances). Characteristics of the synchronous dynamic stiffness around the 1X lateral resonance can be used for early detection of a lateral crack on any rotor. This article describes a study where the torsional and lateral vibrational responses of a rotor with rotating shaft anisotropy due to a transverse crack were modeled.

Notation

D, D_t	Shaft lateral and torsional damping, respectively
I_0	Inboard disk polar moment of inertia
K_x, K_y	Shaft lateral stiffnesses in the "weak" and "strong" directions
$K=(K_x-K_y)/2$	Median stiffness
K_c, K_t	Torsional stiffnesses of coupling and shaft, respectively
M, P	Mass of the outboard disk and radial sideload applied to it
r	Unbalance radius
$q=(K_y-K_x)/2K$	Stiffness anisotropy factor: effect of shaft crack
t	Time
$\gamma=\Omega t-\gamma_0$	Outboard disk angular (torsional mode) coordinate
$\psi=\gamma-\Omega t+\gamma_0$	Outboard disk torsional variable
$v=\sqrt{K/M}$	Lateral mode natural frequency
$v_t=\sqrt{K_t/I_0}$	Torsional mode natural frequency
φ	Inboard disk angular (torsional) coordinate
ω_{n1}, ω_{n2}	Natural frequencies of torsional modes
Ω	Rotative speed

Turbomachinery design changes

The trend to increased efficiency and higher speeds in turbomachinery has resulted in the design of more flexible shafts, which operate at rotative speeds above several of their natural frequencies. Their new design makes them more prone to cracks due to high-cycle and low-cycle fatigue. The accompanying increase in the operating temperatures leads to the shaft's vulnerability to creep and stress corrosion cracking. At least 28 rotor failures due to cracks were documented during the previous ten years in the US power industry [1]. This explains the continuing interest of scientists and engineers in the dynamic behavior and early detection of cracked rotors.

Many published papers have discussed what is considered the major effect of cracked rotors, the lateral response [1-12]. By comparison, the number of papers on torsional vibration due to cracks is significantly smaller [13-15]. Yet, torsional vibrations, especially in resonance conditions, are more sensitive to system dynamic changes because the torsional mode damping, which comes from the shaft material internal friction, is very low.

Of the numerous early cracked shaft cases we studied while monitoring rotating machines in the field, more than 70% of the early warnings have been in synchronous vibration (1X) changes. There is a simple rule, "If the shaft cracks, it is usually bowed, and thus produces a new unbalance situation." The remaining 30% showed activity at the twice rotative speed (2X). Shaft-observing *XY* probes are the best transducer method to monitor rotors. For both 1X and 2X crack symptoms, *either* phase or amplitude changes (not always increasing amplitude) are important. The concept of the "snapping"(accelerated) action when the rotor passes over top dead center, pioneered by the first author of this paper, as a major lateral action, results in the primary coupling from torsional-to-lateral vibrations. The concept of "breathing and gaping cracks," while fine in theory, does not seem to appear in practice. In field cases of cracking shafts, the crack appears to be continuously open.

This article is a continuation of the authors' study of rotor lateral/torsional cross-coupling, due to the shaft crack, unbalance, and radial sideload force. Special attention is paid to the 2X torsional excitation, which is responsible for the rotor "snapping" action, which may intensify crack propagation. A computer simulation of the system enabled the authors to investigate a range of rotor parameters, and the parameters' influence on the rotor lateral and torsional responses.

Mathematical model

The system includes the motor, which is modeled as a source of the regular rotation with rotative speed Ω, connected to the main shaft through the coupling with torsional stiffness and damping K_c and D_c. The main shaft carries two disks and is supported in two relatively rigid bearings. The inboard disk with the polar moment of inertia, I_0, has only

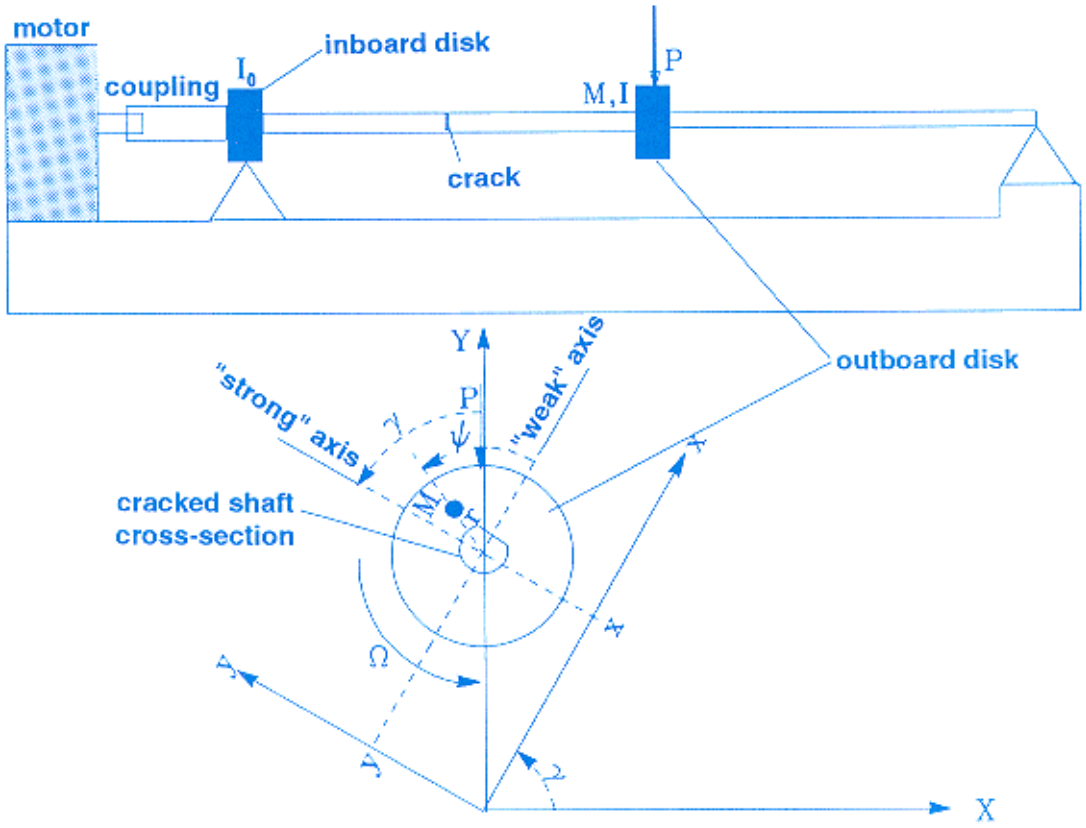

Figure 1
The rotor with simulated transversal crack.

one degree of freedom, described by the angular coordinate, φ (phi).The driving torque is applied to the inboard disk from the motor through the coupling.

The inboard disk is connected to the outboard disk through the shaft, which has a torsional stiffness, K_t and lateral stiffnesses K_x, K_y ($K_x < K_y$). The shaft stiffness anisotropy is caused by added local flexibility due to a crack. The outboard disk has a mass, M, and polar moment of inertia $I = I_0 + r^2M$, where r is the distance between the geometric and mass centers of the disk. The radial sideload, P, is also applied to this disk. The outboard disk motion is described by one torsional coordinate, γ (gamma), and two lateral displacements: x is horizontal and y is vertical in the stationary coordinates. Note that when $\gamma = 0$ or π, the shaft "strong stiffness" axis y passes through the direction of the radial sideload, P. This creates the condition for rotor "snapping" (accelerated) torsional action with all possible damaging consequences. The system has lateral damping, D.

When all cross coupling terms are neglected in the original four-degree-of-freedom model, the rotor torsional modes have the following natural frequencies:

$$\omega_{n1} = \frac{1}{2I_0}\left(2K_t + K_c + \sqrt{K_c^2 + 4K_t^2}\right); \quad \omega_{n2} = \frac{1}{2I_0}\left(2K_t + K_c - \sqrt{K_c^2 + 4K_t^2}\right) \tag{1}$$

Two particular cases, which are important for technical applications, namely, soft and stiff coupling, are discussed below.

2.1) ***Soft coupling:*** $K_t / K_c > 1$

In this case, the first torsional mode represents the twist angle between the inboard and outboard disks, and has a natural frequency of approximately $\sqrt{2K_t / I_0}$. The second mode represents an angular motion of the main shaft as the rigid body, and has a natural frequency of approximately $\sqrt{K_c / (2I_0)}$. This is less important in practical applications.

2.2) ***Stiff coupling:*** $K_t / K_c << 1$

In this case, the first torsional mode represents an angular displacement of the inboard disk, and has a natural frequency of approximately $\sqrt{K_c / I_0}$ The second mode represents an angular displacement of the outboard disk, and has a natural frequency of approximately $\sqrt{K_t / I_0}$ ($\omega_{n1} >> \omega_{n2}$). For frequencies below the first natural frequency, the angular coordinate of the inboard disk describes the regular rotation ($\varphi = \Omega t$). The investigation below considers this particular case.

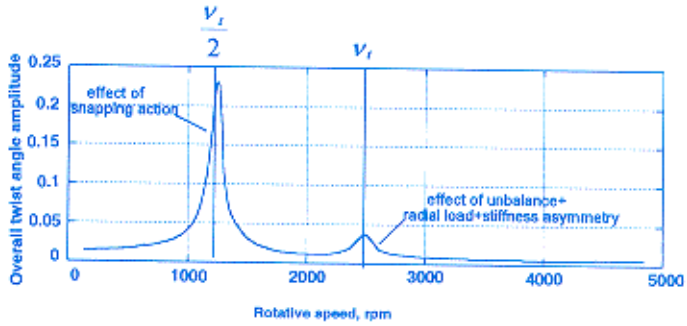

Figure 2
Overall amplitude of the rotor torsional response obtained from the computer simulation of case (a).

Numerical simulation and analysis

The computer model of the described rotor was built. Three sets of parameters used in the numerical simulation are presented in Table 1 (see Notation):

Since the numerical integration was performed in the range of rotative speeds from 0 to 5000 rpm, case (a) obviously does not experience any significant lateral motion activity, except static lateral displacement due to the radial sideload. The only important equation for the outboard disk torsional vibration is simplified to the following:

$$\ddot{\psi} + \frac{D_t}{I_0}\dot{\psi} + \frac{K_t}{I_0}\psi = \frac{qPr}{I_0}\cos(\Omega t + \psi - \gamma_0) + \frac{qP^2}{KI_0}\sin\{2(\Omega t + \psi - \gamma_0)\} \tag{2}$$

where γ_0 is a stationary component of the angle γ, $\psi = \gamma - \Omega t + \gamma_0$.

Eq. (2) can be considered as a linear oscillator with two forcing terms: 1X excitation due to the combination of unbalance, shaft stiffness asymmetry, and radial sideload, and 2X excitation due to the shaft stiffness asymmetry and radial sideload. The latter excitation results in the effect called the "snapping" action: the torque experiences two positive peaks when the strong stiffness axis passes the radial sideload direction with the angle 45° (i.e., $\gamma = \Omega t + \psi - \gamma_0 = \frac{\pi}{4}$ or $\frac{5\pi}{4}$). The results of the numerical simulation for case (a) are presented in the form of overall torsional amplitude versus rotative speed (Fig. 2). Note that the effect of the synchronous excitation is relatively small due to the low amount of unbalance. 1X and 2X filtered torsional responses are shown in Figure 3, indicating that two peaks in Figure 2 are, indeed, 2X and 1X resonances.

	v[cpm]	v_t [cpm]	q	r[in]	$\frac{P}{M}$, [in / sec^2]	$\frac{D}{\sqrt{KM}}$	$\frac{D_t}{\sqrt{I_0 K_t}}$
Case (a)	15000	2500	0.2	0.05	60000	0.2	0.04
Case (b)	1700	15000	0.2	0.001	1000	0.2	0.04
Case (c)	1700	2500	0.2	0.001	1000	0.2	0.04

Table 1
The Main Parameters of the Rotor System Numerical Simulation.

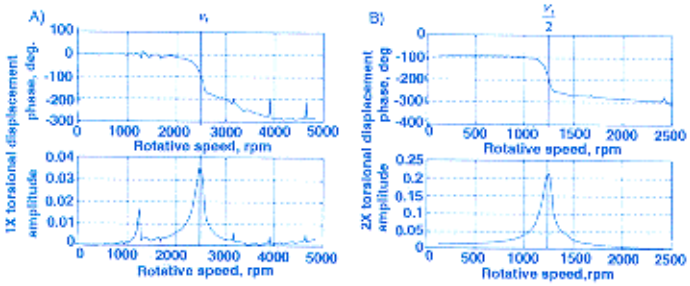

Figure 3
Bode plots of the torsional response of the rotor for case (a).
A) 1X filtered response. B) 2X filtered response.

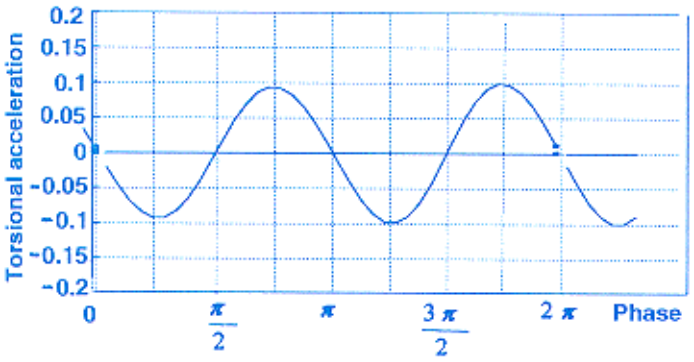

Figure 4
The waveform of the rotor torsional acceleration
at $\Omega = 1000$ rpm for case (a).

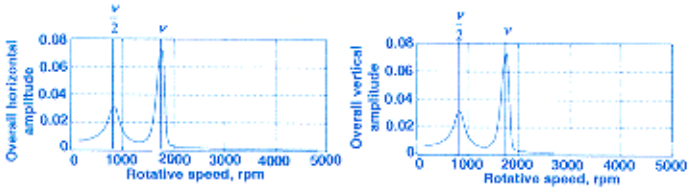

Figure 5
Overall amplitudes of the rotor horizontal and
vertical responses for case (b).

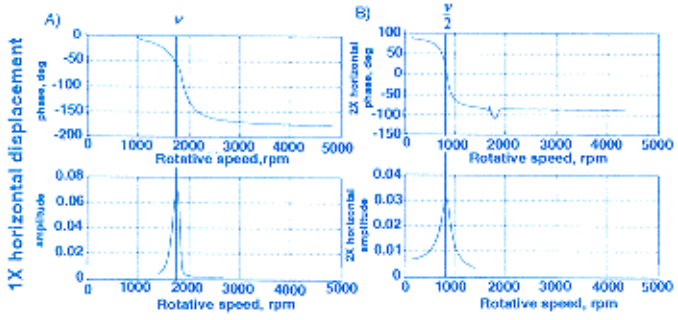

Figure 6
Bode plots of the horizontal response of the rotor for case (b).
A) 1X filtered response. B) 2X filtered response.

The torsional acceleration timebase waveform (Figure 4) at the rotative speed $\Omega = 1000$ rpm (close to the 2X resonance at $\Omega = 1250$ rpm) illustrates the fact that, due to the snapping action, the torque experiences two positive peaks when $\gamma = \frac{\pi}{4}$ and $\frac{5\pi}{4}$. The Keyphasor® (once-per-turn marker) position here corresponds to $\gamma = 0$, when the strong axis coincides with the direction of the radial sideload. Note that, since the waveform was taken below the 2X resonance, the torsional acceleration lags the excitation by π, and has negative peaks while the snapping torque has positive ones.

Case (b) (Table 1) is, in a sense, an opposite to case (a); in the rotative speed range (0 to 5000 rpm), due to stiff coupling, the rotor does not exhibit any significant torsional activity. The rotor lateral response for this case, obtained by the computer simulation, is shown in Figure 5 in the form of overall vertical and horizontal vibration response amplitudes. Together with 1X and 2X Bode plots in Figure 6, they confirm that, in the case of a significant difference in the lateral and torsional natural frequency values, there is almost no interaction between the modes, and the lateral response consists of mainly 1X and 2X components. The Bode plots of 1X and 2X filtered vertical and horizontal responses of the rotor are almost identical (Figure 5).

Case (c) overlaps the first two cases. Both lateral and torsional natural frequencies are in the range of the considered rotative speeds; therefore, the case is expected to exhibit both lateral and torsional vibrational activities. The results of this case simulation are presented in the form of lateral and torsional overall amplitudes versus rotative speed (Figures 7 and 8).

Note that the overall lateral amplitudes for case (c) are practically identical to those of case (b). The same holds true for 1X and 2X filtered vertical and horizontal responses. (They are not displayed here.)

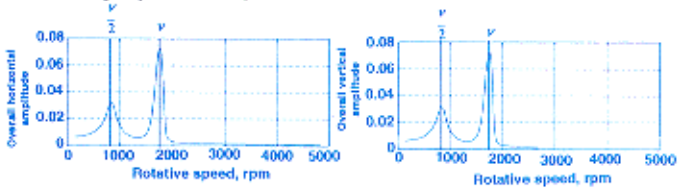

Figure 7
Overall amplitudes of the rotor horizontal and
vertical responses for case (c).

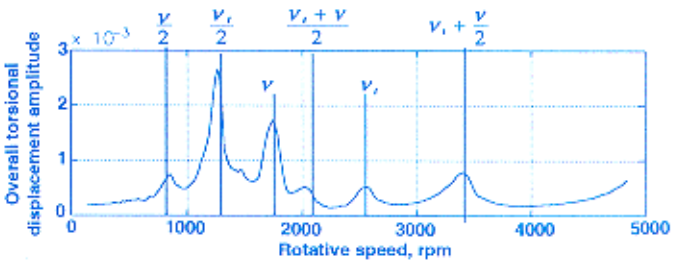

Figure 8
Overall amplitude of the rotor torsional response for
case (c). Compare with Figure 5.

As is shown in Figure 8, the situation is now different for the rotor torsional response. In addition to the amplitude peaks occurring at $\Omega = \frac{v_t}{2}$ and v_t, which were present in Figure 2 for case (a), the torsional response of the rotor for case (c) exhibits 1X and 2X lateral resonances at $\Omega = v$ and $\frac{v}{2}$, respectively. The existence of fractional combination resonances, due to nonlinear coupling, is also shown at $\Omega = \frac{v_t + v}{2}$ and $v_t + \frac{v}{2}$. Figure 9 presents Bode plots of the 1X and 2X filtered torsional responses for case (c). The peaks at $\Omega = v$ and v_t are due to the 1X lateral and torsional resonances, respectively, and overall peaks at $\Omega = \frac{v}{2}$ and $\frac{v_t}{2}$ are due to the 2X lateral and torsional resonances.

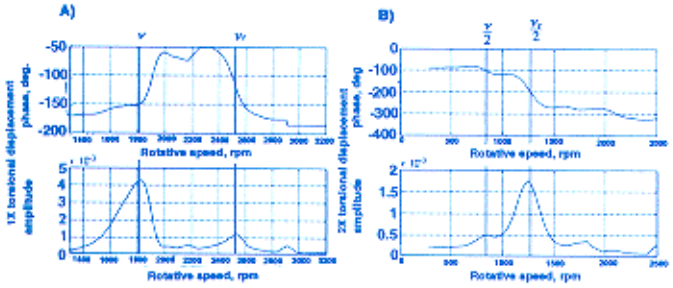

Figure 9
Bode plots of the torsional response of the rotor for case (c).
A) 1X filtered response. B) 2X filtered response.

Analytical consideration

The analysis of the full system of four lateral/torsional nonlinearly coupled equations of motion shows the possibility of the sequence of resonances, as is summarized in Table 2.

As is shown in Table 2, the rotor system without stiffness asymmetry ($q = 0$) allows for main lateral and integer combination lateral and torsional resonances due to the unbalance. The stiffness asymmetry, q, by itself compliments torsional resonances and fractional combination resonances of the first group. Its product with radial sideload affects all the resonances of the system. According to Figure 8, the torsional response of the rotor for case (c) shows fractional combination resonances of group 2, which are due to the product $q\,P/K$.

As was mentioned in the introduction, in 70% of successful early detection of cracks, the warnings were received from a 1X lateral rotor response change. That makes the investigation of the stiffness asymmetry influence on the 1X lateral response the most important. The mathematical analysis of the lateral motion equations in the region around 1X lateral resonance, supported by the numerical simulation, provides the results presented in Figure 10. They are in the form of a 1X Bode plot and components of the system synchronous dynamic stiffness.

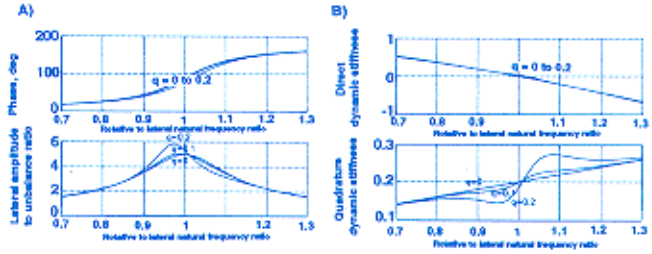

Figure 10.
A) Bode plot of the rotor 1X lateral response in the range of rotative speeds close to the lateral natural frequency for the cases of $q = 0, 0.1, 0.2$.

B) Nondimensional direct and quadrature synchronous dynamic stiffnesses in the range of rotative speeds close to the rotor lateral natural frequency for the cases $q = 0, 0.1, 0.2$.

Resonance frequency relations	Names of the resonances	Terms responsible for the resonance are proportional to:
$m = 1,\ \Omega = v$	Main lateral resonance	$r, qP/K$
$m = \frac{1}{2},\ \Omega = \frac{v}{2}$	Fractional lateral resonance	qP/K
$m = kn,\ \Omega = kv_t,\ m = \left(k - \frac{1}{2}\right)n,\ \Omega = \left(k - \frac{1}{2}\right)v_t,\ (k = 1,2,3\ldots)$	Torsional resonances	$q,\ qP/K, q(p/K)^2$
$m = kn - 1,\ \Omega = kv_t - v,\ m = 1 \pm kn,\ \Omega = v \pm kv_t,\ (k = 1,2,3\ldots)$	Integer combination resonances	$r,\ q,\ qp/K$
$m = \left(k - \frac{1}{2}\right)n \pm 1,\ \Omega = \left(k - \frac{1}{2}\right)v_t \pm v,\ m = 1 - \left(k - \frac{1}{2}\right)n,\ \Omega = v - \left(k - \frac{1}{2}\right)v_t,\ (k = 1,2,3\ldots)$	Fractional combination resonances (group 1)	$q, qp/K$
$m = \frac{1}{2} \pm kn,\ \Omega = \frac{v}{2} \pm kv_t,\ m = kn \pm \frac{1}{2},\ \Omega = kv_t - \frac{v}{2},\ m = \frac{1}{2} \pm \left(k - \frac{1}{2}\right)n,\ \Omega = \frac{1}{2} \pm \left(k - \frac{1}{2}\right)v_t$ $m = \left(k - \frac{1}{2}\right)n - \frac{1}{2},\ \Omega = \left(k - \frac{1}{2}\right)v_t - \frac{v}{2},\ (k = 1,2,3\ldots)$	Fractional combination resonances (group 2)	$q\,p/K$

Table 2
The list of possible lateral and torsional resonances

It is obvious that the synchronous dynamic stiffness depends on the unbalance angular orientation related to the shaft weak and strong stiffness directions. Note that in Figure 10 the change of the stiffness asymmetry factor, *q*, from 0 to 0.2 has a very small effect on the phase lag, but the amplitude peak changes noticeably.

As follows from Figure 10B, the stiffness asymmetry primarily affects the quadrature dynamic stiffness in the region close to the main lateral resonance. Since the synchronous dynamic stiffness is the reciprocal of the influence vector used in the balancing, the information about its behavior is often available, and can be used in diagnostics of rotating machine health, and early detection of rotor cracks in particular.

Closing Remarks

A simple rotor system with a shaft transverse crack was considered in this article. The lateral and torsional modes interact with each other, due to the rotor unbalance, radial sideload, and rotating asymmetry. In the absence of any torsional excitation from the driving and load torques, the rotor torsional vibrations show noticeable 1X and 2X resonances. This effect was confirmed experimentally [15]. The main source of the torsional excitation was related to the torsional snapping action due to the radial sideload. The snapping action can be defined as a periodic (twice per rotation) elastic energy storage occurring when the shaft strong axis approaches the radial sideload direction, followed by its release when the rotor weak stiffness axis passes through the radial sideload direction.

In addition to the above source of 2X excitation, 1X exciting torque also exists, due to the combination of the rotor unbalance, stiffness asymmetry, and radial sideload. Due to coupling, the torsional response exhibits 1X and 2X lateral resonances. The existence of additional fractional combination resonances was numerically found and analytically explained.

The torsional response timebase waveform observation in the range around 2X torsional resonance (Figure 4) allows for an estimation of the crack angular orientation. The torsional response also reflects 1X and 2X lateral resonances. The lateral response of the system was not noticeably affected by the torsional vibration, and consisted primarily of 1X and 2X components. (The lateral mode carries more damping.) The synchronous dynamic stiffness components in the proximity of the 1X lateral resonance revealed that the shape of the quadrature component is most sensitive to the shaft stiffness asymmetry. This information can be used for shaft crack detection. The latter conclusion can easily be applied directly in the field, since the information on the synchronous dynamic stiffness is usually available from influence vectors used in balancing.

Rotating machinery designers are normally cautious when lateral and torsional resonance frequencies aren't close to each other and when the operating speed isn't close to either the lateral or torsional resonance frequencies or their half values. The cracked shaft lateral and torsional response described in this article strongly suggests not having lateral resonance frequency close to half of the torsional resonance and vice versa. If one of these conditions is violated, the pending crack will lead to high amplitudes of both lateral and torsional vibrations, as a consequence of the high level of normal and shear stresses in the rotor. The torsional resonance amplitudes are usually much higher than the lateral ones, due to very low damping in the rotor torsional mode. Any system changes due to a shaft crack, therefore, would be better reflected in torsional than lateral vibration changes. ■

Glossary of terms

Anisotropic - having properties, such as stiffness or conductivity, which vary according to the direction in which they are measured.

Combination resonances - the coincidence of excitation frequency with the integer and fractional combination of two or more natural frequencies of the rotor system.

Torsional vibration - time variation of the angle of twist, of a shaft or beam, typically measured in tenths of degrees pp.

Transversal crack - a crack which is perpendicular to the longitudinal axis of the rotor.

1X - In a complex vibration signal, the notation for the signal component that has frequency equal to the rotative speed. Also called synchronous.

2X, 3X, etc. - In a complex vibration signal, the notation for signal components having frequencies equal to exact multiples of shaft rotative speed. Also called higher harmonics, superharmonics.

References

1 Bently, D. E., Muszynska, A., "Detection of Rotor Cracks," Proceedings of 15th Turbomachinery Symposium, Corpus Christi, Texas, Nov. 1986, pp. 129-139.

2 Dimentberg, F. M., "Flexural Vibration of Rotating Shafts," Butterworth, London, 1961.

3 Henry, T. A., Okah-Avae, B. E., "Vibrations in Cracked Shafts," Vibrations in Rotating Machinery, Inst. of Mech. Eng., London, 1976, pp. 15-19.

4 Mayes, I. W., Davies, W. G. R., "The Vibrational Behavior of a Rotating Shaft System Containing a Transverse Crack," IMechE. Conference, Paper C178/76,1976.

5 Gasch, R., "Dynamic Behavior of a Simple Rotor With a Cross-Sectional Crack," Vibrations in Rotating Machinery, Inst. of Mech. Eng., London, 1976, pp. 123-128.

6 Grabowski, B., "The Vibrational Behavior of a Turbine Rotor Containing a Transverse Crack," J. Mech. Des., Vol. 102, 1979, pp. 15-19.

7 Inagaki, Y., Kanaki, H., Shiraki, K., "Transverse Vibrations of a General Cracked Rotor Bearing System," ASME Paper 81-DET-45, 1981.

8 Muszynska, A., "Shaft Crack Detection," Seventh Machinery Dynamics Seminar, Canada, 1982.

9 Nelson, H. D., Nataraj, C., "The Dynamics of a Rotor System with a Cracked Shaft," ASME J. Vibration, Acoustics, Stress and Reliability in Design, Vol. 108, No. 2, 00, pp. 189-196.

10 Chen, W. H., Wang, H. L., "Finite Element Analysis of Axisymmetric Cracked Solid Subjected to Torsional Loadings," Eng. Frac. Mech., Vol. 23, No. 4, 1986, pp. 705-717.

11 Dirr, B. O., Schmalhorst, B. K., "Crack Depth Analysis of a Rotating Shaft by Vibration Measurement," 11th ASME Conf. Vib. Noise, Boston, DE v. 2, 1987, pp. 607-614

12 Qian, G., Gu, S., Jiang, J., "Finite Element Model of Cracked Plates Application to Vibration Problem," Comput. Str., 39, 5, 1991, pp. 483-487.

13 Cohen, R., Porat, I., "Coupled Torsional and Transverse Vibration of Unbalanced Rotor," J. of Applied Mechanics, 1985, Vol. 52, No. 9, pp. 701-705.

14 Christides, S., Barr, A. D. S., "Torsional Vibration of Cracked Beams of Non-Circular Cross-Section," Int. J. Mech. Sci., Vol. 28, No. 7, 1986, pp. 473-490.

15 Muszynska, A., Goldman, P., Bently, D. E., "Torsional /Lateral Cross-Coupled Responses Due to Shaft Anisotropy: A New Tool in Shaft Crack Detection," IMechE, C 432-090, Bath, United Kingdom, 1992.